GALACTO-FORENSIC OF LMC'S ORBITAL HISTORY AS A PROBE FOR THE DARK MATTER POTENTIAL IN THE OUTSKIRT OF THE GALAXY

Xiaojia Zhang[1,2*], Douglas N. C. Lin[2,3], Andreas Burkert[4,5,6], Ludwig Oser,[7]
Draft version September 19, 2012

ABSTRACT

The 3D observed velocities of the Large and Small Magellanic Clouds (LMC and SMC) provide an opportunity to probe the Galactic potential in the outskirt of the Galactic halo. Based on a canonical NFW model of the Galactic potential, Besla et al.(2007) reconstructed LMC and SMC's orbits and suggested that they are currently on their first perigalacticon passage about the Galaxy. Motivated by several recent revisions of the Sun's motion around the Galactic center, we re-examine the LMC's orbital history and show that it depends sensitively on the dark-matter's mass distribution beyond its present Galactic distance. We utilize results of numerical simulations to consider a range of possible structural and evolutionary models for the Galactic potentials. We find that within the theoretical and observational uncertainties, it is possible for the LMC to have had multiple perigalacticon passages on the Hubble time scale, especially if the Galactic circular velocity at the location of the Sun is greater than ~ 228km s^{-1}. Based on these models, a more accurate determination of the LMC's motion may be used to determine the dark matter distribution in the outskirt of the Galactic halo.

1. INTRODUCTION

The Large and Small Magellanic Clouds (LMC and SMC) are the two most prominent satellite galaxies in the Local Group. They are accompanied by the Magellanic Stream which extends along a great circle over 100 degrees across the sky. One end of the Stream joins, both in position and radial velocity, onto the bridge between the LMC and SMC (Meatheringham et al 1988). A continuous velocity gradient leads to a large infall speed at the other end of the Stream (Mathewson, Cleary, & Murray 1974).

The kinematic properties of the LMC, SMC, and the Magellanic Stream have motivated many investigations on their origin. One class of models are based on the assumption that the Stream is the tidal debris of the LMC and SMC during their past perigalacticon passages (Toomre 1972, Mirabel & Turner 1973, Fujimoto & Sofue 1976, Lynden-Bell & Lin 1977, Murai & Fujimoto 1980, Gardiner et al 1994, Putman et al 1999). Numerical simulations with idealized Galactic potentials have led to the prediction for the LMC's proper motion to be 0.02″ per century in a direction such that it leads the Magellanic Stream (Lin & Lynden-Bell 1982). A subsequent ground-based observational confirmation gave a slightly smaller value (Jones et al 1994, Lin et al 1995). Nevertheless, the tidal scenario has been challenged by the lack of excess halo stars in the direction of the Stream (Majewski et al.

* E-mail: xiaojia.f.zhang@gmail.com
[1] Department of Astronomy, Peking University, Beijing 100871, China
[2] Kavli Institute for Astronomy and Astrophysics, Peking University, Beijing 100871, China
[3] Department of Astronomy and Astrophysics, University of California, Santa Cruz, CA 95064, U.S.A.
[4] University Observatory Munich, Scheinerstrasse 1, D-81679 Munich, Germany
[5] Max-Planck-Institute for Extraterrestrial Physics, Giessenbachstrasse 1, 85758 Garching, Germany
[6] Max-Planck Fellow
[7] Max-Planck-Institute for Astrophysics, Karl-Schwarzschild-Str. 1, D-85741 Garching. Germany

2003) since in such a model, stars and gas should have been equally stripped from the Magellanic Clouds. Some of these issues may be resolved with an alternative scenario that the gas in the Magellanic Stream was removed from the LMC by a ram pressure as it ploughed through the hot residual gas in the Galactic halo (Moore & Davis 1994). The density of the halo gas must be sufficiently high to remove atomic gas from the LMC. It also needs to be sufficiently tenuous to avoid any drag on the Stream and reduction of its infall speed below its observed values (Mastropietro et al 2005).

One possible test to distinguish between these scenarios is to reconstruct the LMC's orbital history with a set of accurate observational data. The proper-motion measurements by Kallivayalil et al.(2006a, 2006b) made with the Hubble Space Telescope (HST) provided a set of accurate 3D Galactocentric velocities for both LMC and SMC. After correcting for the motion of the Sun (they adopted a Galactic circular velocity, at the Sun's location, of $V_c = 220$km s^{-1}), they obtained a transverse velocity of the LMC to be ~ 367km s^{-1} which is much larger than the inferred Galactic circular velocity at its present-day location and its radial velocity which has a positive, modest value of ~ 89km s^{-1}.

The newly obtained 3D velocity data confirm that the LMC has just passed its perigalacticon. They are also useful for the reconstruction of the LMC's orbital history especially at the time of its previous perigalactic passage. But, such a determination depends on the prescription for the Galactic potential. For example, Lin & Lynden-Bell (1982) adopted an idealized model which is almost certain over simplified. Although, the most recently measured proper motion is in agreement with their prediction, to within a second decimal place, LMC's orbit needs to be re-examined with a more appropriate Galactic potential. Using these velocities and a ΛCDM-motivated MW model with the virial radius ($R_{vir} = 258kpc$) and mass ($M_{vir} = 10^{12}M_\odot$), Besla et al.(2007) reconstructed the orbital history of the Clouds and suggested that they

are on their first passage about the MW.

The first-passage conclusion obtained by Besla et al.(2007), if verified, would invalidate the tidal origin of the Magellanic Stream. In a follow-up investigation, Besla et al. (2010) suggested that gas in the Magellanic Stream was torn from the SMC by the tide of LMC before the two Clouds impinged to the apogalacticon. To match the observed column density along the Stream, they adopted a gas to star (and dark matter) mass ratio for the SMC to be an order of magnitude larger than those they adopted for the LMC. In order to distinguish these alternative scenarios, it is desirable to check the robustness of their results.

We begin with a re-analysis of the kinematic data. At the Clouds' present-day position in the sky, a large fraction of their observed line of sight and proper motion speeds are due to the Sun's motion around the Galactic center. The distance of the Sun from the Galactic center and the circular velocity of the local standard of rest have been revised recently (Reid et al. 2009a) to be $R_0 = 8.4 \pm 0.6 kpc$ and $V_c = 254 \pm 16 \mathrm{km\ s^{-1}}$ respectively. These latest determinations are based on the reference frame set by the maser sources near the Galactic center. In §2, we show that this new value of V_c modifies the correction of the solar motion and LMC's 3D speed. It also significantly revises the reconstruction of the Magellanic Clouds' orbital history (see a similar conclusion by Shattow & Loeb 2009).

But, there are other recent analysis which lead to a range of values for V_c's. Based on 18 precisely measured Galactic masers, Bovy et al (2009) deduced a lower estimation for the circular velocity at the Sun's location to be $V_c = 236 \pm 11 \mathrm{\ km\ s^{-1}}$. In another APOGEE analysis, Bovy et al (2012) concluded $V_c = 218 \pm 6 \mathrm{\ km\ s^{-1}}$ and claimed that $V_c < 235 \mathrm{\ km\ s^{-1}}$ at $> 99\%$ confidence level. In light of this range of V_c, we will discuss, in §4.2, the dependence of the LMC's orbital history on V_c within an error bar.

A high value (254 km s^{-1}) of V_c also indicates that the rotation curve of the Milky Way Galaxy is similar to that of the Andromeda Galaxy, suggesting they may have comparably massive dark matter halos. Their combined masses can be estimated from the timing argument (Kahn & Woltjer, 1959) because these two most prominent galaxies in the Local Group are currently approaching each other and they are presumably bound to each other. Based on a recent measurement of M31's proper motion, van der Marel et al (2012) estimate a total mass of the Local Group to be $3 \sim 4 \times 10^{12} M_\odot$. If their kinematic properties are very similar to each other, the mass of either the Milky Way or M31 would be $1.5 \sim 2 \times 10^{12} M_\odot$. This mass is mostly in the form of a dark matter halo. In order to verify this possibility, we re-analyze the space motion of the LMC based on this new information. We briefly recapitulate the equation of motion in §2.

In §3, we illustrate that the LMC's orbital history also depends sensitively on the mass distribution in the outer Galactic halo, over and above the uncertainties introduced by the magnitude of V_c. As an illustration, we prescribe the Galactic potential as $\Phi \propto r^{-\lambda}$ $(0 < \lambda < 1)$ and show that if $\lambda \sim 0.1$, the LMC would be currently on its second passage about the Milky Way. It is useful to

adopt a more realistic Galactic potential and determine the history of the LMC's orbit.

There are several attempts to reconstruct the Galactic potential based on the velocity information of satellite galaxies (Peebles 2001, 2010). However these determinations are highly uncertain. We follow the approach of Besla et al (2007) by utilizing an idealized potential based on the ΛCDM simulations. These simulations produce to well determined profiles for the density distribution in the inner regions of galaxies (Navarro et al. 1997, hereafter NFW). However, our illustrative model indicates that LMC's past orbit sensitively depends on the potential in the outer regions of the galaxy. Numerical simulations show that there are considerable uncertainties and dispersion in the mass distribution for outer regions of galaxies.

In order to explore the possible range of the LMC's orbital history, we select, in the §4, several sample dark-matter halos of galaxies from numerical CDM simulations. These models have slight variations in the slope of the dark matter density distribution. We also take into consideration that with the revised circular velocity of the Sun's motion, the mass of the Galaxy may need to be upgraded to be comparable to that of M31. With the simulated profile of the Galactic potential, we show that it is possible for the LMC to have had several encounters with the Galaxy. Since the mass ratio between the LMC and SMC is 10 : 1, we neglect SMC's contribution. In §5, we summarize our results and discuss their implications.

2. ORBITAL PARAMETERS

2.1. *LMC's spacial velocity*

In their investigation, Kallivayalil et al. (2006a) used $V_{c,sun} = 220 \mathrm{km\ s^{-1}}$ as the circular velocity of the Sun. (This value is similar to that derived by Bovy et al. 2012). They followed the method outlined in van der Marel et al. (2002), and obtain the LMC's total, radial, and azimuthal velocities as: $v_{LMC} = 378 \pm 18 \mathrm{km\ s^{-1}}$, $v_{LMC,rad} = 89 \pm 4 \mathrm{km\ s^{-1}}$, and $v_{LMC,azi} = 367 \pm 18 \mathrm{km\ s^{-1}}$ respectively. Here we adopt the same procedure to correct for the solar motion, including the Sun's peculiar motion relative to the local standard of rest determined by Dehnen & Binney (1998) as $(U_\odot, V_\odot, W_\odot) = (10.0 \pm 0.4, 5.2 \pm 0.6, 7.2 \pm 0.4) km/s$, and apply the recently revised $V_{c,sun} \sim 250 \mathrm{km\ s^{-1}}$ (Reid et al. 2009a) to compute the LMC's total, radial, and azimuthal velocities. We adopt this high value for $V_{c,sun}$ to illustrate that it can significantly modified the deduced orbital history of the Magellanic Clouds (also see, Shattow & Loeb 2009). For this revised value of the solar motion we find values of $v_{LMC} \sim 356 \mathrm{km\ s^{-1}}$, $v_{LMC,rad} \sim 63 \mathrm{km\ s^{-1}}$, and $v_{LMC,azi} \sim 351 \mathrm{km\ s^{-1}}$ respectively.

2.2. *LMC's equation of motion*

All of the new kinematic quantities (derived with the newly revised $V_{c,sun}$ are one sigma smaller than their previously determined values and they are expected to imply a more bound LMC's orbit around the Galaxy. In order to verify this expectation, we compute the LMC's orbital history.

Under the influence of the Galactic potential and dy-

namical friction, LMC's equation of motion is

$$\ddot{\mathbf{r}} = \frac{\partial}{\partial \mathbf{r}} \Phi(r) + \frac{\mathbf{F}_{DM}}{M_{LMC}}. \tag{1}$$

We adopt the idealized Chandrasekhar(1943) formula for dynamical friction such that

$$\mathbf{F}_{DM} = -\frac{4\pi ln\Lambda G^2 M_{LMC}^2 \rho(r)}{V_{LMC}^3} [erf(X) - \frac{2X}{\sqrt{\pi}} e^{-X^2}] \mathbf{V}_{LMC} \tag{2}$$

where $X \equiv V_{LMC}/\sqrt{2}\sigma$, σ is the velocity dispersion of the DM halo and $\rho(r)$ is the density of the halo at r. For the present application, we neglect the effect of an active halo and mass loss from the LMC (Fellhauer & Lin 2007). The mass of the LMC is about $2 \times 10^{10} M_\odot$. In most previous applications, the Coulomb logarithm in the above formula is assumed to be a constant $\Lambda = b_{max}/b_{min}$ (Binney and Tremaine 1987). Here we use a prescription introduced by Hashimoto et al.(2003) in which b_{max} is replaced by the position of the satellite and $b_{min} = 4.8kpc$. After the specification of the Galactic potential, equation (1) can be solved numerically with a symplectic leapfrog integration scheme(Springel et al. 2001). We verify the numerical accuracy with a range of time steps. For typical models, several hundred steps per orbit are more than sufficient for numerical convergence.

3. DEPENDENCE ON POTENTIAL MODEL OF THE MILKY WAY

We first show the sensitive dependence of the LMC's orbital period on the Galactic potential. For illustration purpose, we adopt a spherically symmetric, static model with a power law potential profile for the Galactic potential.

3.1. A simple power law profile

At LMC's Galactocentric distance, the local circular velocity is much larger than its radial velocity and smaller than its transverse velocity, and the radial velocity is positive. These kinematic properties suggest that the LMC has just passed its perigalacticon. Since the LMC is close to its perigalacticon, its orbital history is mainly related to the structure of the Galaxy outside the perigalacticon distance of LMC. Therefore, we mainly focus on the outer part of the Galaxy in order to estimate how the orbital period of the LMC depends on the model parameters.

We assume an idealized power-law potential $\Phi \propto r^{-\lambda}(0 < \lambda < 1)$. The gravity felt by the LMC at a distance r is

$$F(r) = \frac{GM(r_p)M_{LMC}}{r_p^2} \left(\frac{r}{r_p}\right)^{-\lambda-1} \tag{3}$$

where r_p is the perigalacticon distance of the LMC in Galactocentric Coordinates and $M(r_p)$ is the total mass of the Galaxy inside r_p. Integrate this force to get the potential of the Galaxy beyond r_p:

$$\Phi(r) = \Phi(r_p) \left(\frac{r}{r_p}\right)^{-\lambda} = \frac{1}{\lambda} \frac{GM(r_p)}{r_p} \left(\frac{r}{r_p}\right)^{-\lambda} \tag{4}$$
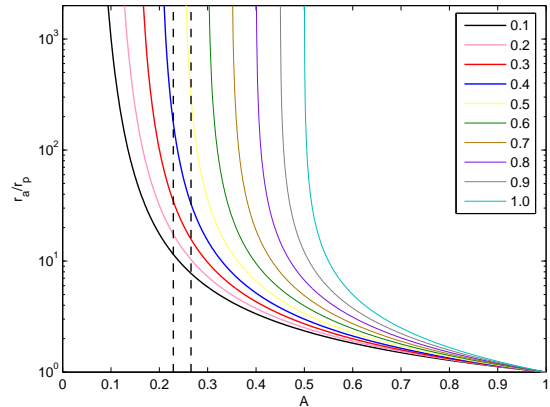

FIG. 1.— The dependence of ratio r_a/r_p on A with different values of λ. From below to above the 10 lines corresponds to λ from 0.1 to 1.0 respectively. The two vertical dashed lines represent the value span of A from 0.229 to 0.265 corresponding to $V_t = 378km/s$ to $351km/s$ for LMC.

Under the conservation of energy and angular momentum,

$$\frac{1}{2} \left[1 - \left(\frac{1-e}{1+e}\right)^2 \right] \left[1 - \left(\frac{1-e}{1+e}\right)^\lambda \right]^{-1} = \frac{\Phi(r_p)}{v_t^2} \tag{5}$$

where the orbital eccentricity is defined such that $r_p/r_a = (1-e)/(1+e)$, v_t is the tangential velocity of the LMC at r_p. Substitute $\Phi(r_p)$ and define:

$$A(e, \lambda) \equiv \frac{\lambda}{2} \left[1 - \left(\frac{1-e}{1+e}\right)^2 \right] \left[1 - \left(\frac{1-e}{1+e}\right)^\lambda \right]^{-1}$$
$$= \frac{GM(r_p)}{v_t^2 r_p} = \frac{v_c(r_p)^2}{v_t^2}. \tag{6}$$

In the above equation, the magnitude of A is determined by the LMC's azimuthal velocity and distance at perigalacticon. For a given λ, each value of A implies a set of values for e, r_a, and orbital period (see fig 1). For a given value of λ, r_a/r_p would decrease rapidly with increase of A if the LMC's eccentricity is high. It would also decrease rapidly with decreasing value of λ if the value of A is close to the minimum value required for a bound orbit. These tendencies imply that, in the limitation of high eccentricity, a small modification in the value of e (due to fractional changes in the values of A or λ) would lead to very different orbital periods.

The derivation of equation (6) is based on the assumed conservation of energy and angular momentum. Had we taken into account the effect of dynamical friction, the loss of energy and angular momentum in time would imply a larger apogalacticon distance and a longer orbital period in the past, albeit the magnitude of its contribution is modest. The uncertainties of the LMC's transverse velocity v_t and mass distribution of the Galaxy are contained in the values of A and λ. In the previous section, we have already discussed the potential reduction in the value of v_t due to an upward revision in the value of $V_{c,sun}$. For a given value of λ, the corresponding increase in A (eq. 6) would reduce the values of r_a/r_p (Fig. 1) and LMC's Galactic orbital period.
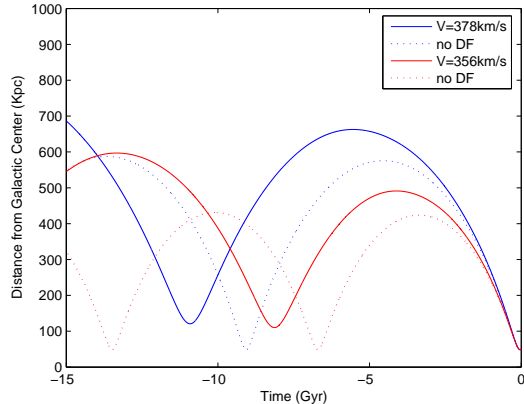
FIG. 2.— The dependence of orbital history on the LMC's velocity with $\lambda = 0.1$. The dotted lines are the results without dynamical friction. Both velocities would lead to more than one passages during Hubble time even with under the influence of a strong dynamical friction effect.

Adopting the most recently revised circular velocity of the local standard of rest and LMC's location ($r_p \sim 50kpc$) as v_t and r_p, equation (1) can be solved for different values of λ. In order to illustrate this point, we choose $\lambda = 0.1$ and $M(r_p) = 3.8 \times 10^{11} M_\odot$ (model A_1 of Klypin et al. 2002) to examine the orbital history. This value of $M(r_p)$ is identical to that used by Besla et al (2007). With these parameters the corresponding value of A for LMC is 0.229 and 0.65 under the tangential velocity as $V_t = 378km/s$ and $V_t = 351km/s$ respectively(Fig. 1). We choose a small value for λ because if the rotation curve remains relatively flat in the outside part of the Galaxy, λ would be very close to zero.

In order to determine the magnitude of dynamical friction from equation (2), we adopt the density distribution of the Galactic dark matter halo from equation (4). We choose the largest value (1) for X. This approximation slightly over-estimates the contributions from the dynamical friction. With this form of the potential, we obtain more than one past perigalacticon passage by the LMC for both the previous (which yields $v_t = 378$km s^{-1}) and the latest solar circular velocities (which yields 356km s^{-1}) (Figure 2). The smaller magnitude of the newly determined azimuthal speed decreases the LMC's orbital period significantly as expected.

4. NFW MODEL AND SIMULATION DATA

4.1. *Models of Galactic potential*

In order to construct a more realistic Galactic potential, we separate the baryonic and dark matter contribution to the Galactic potential such that

$$M(r) = M_b(r) + M_{dm}(r) \qquad (7)$$

We assume that the dark matter density profile is described by a NFW model (Navarro et al. 1997):

$$\rho_{halo}(r) = \frac{\rho_s}{x(1+x)^2}, \qquad x = \frac{r}{r_s}, \qquad (8)$$

$$M_{halo}(r) = 4\pi\rho_s r_s^3 f(x) = M_{vir} f(x)/f(C) \qquad (9)$$

$$f(x) = ln(1+x) - \frac{x}{1+x} \qquad (10)$$

$$C = r_{vir}/r_s \qquad (11)$$

$$M_{vir} = \frac{4\pi}{3}\rho_{cr}\Omega_M \delta_{th} r_{vir}^3 \qquad (12)$$

In the above equations, C is the halo concentration, M_{vir} and r_{vir} are the halo virial mass and radius. The ρ_{cr} is the critical density of the universe and δ_{th} is the overdensity of a collapsed object according to the spherical top-hat model(Gunn & Gott 1972). The r_{vir} is defined as the radius inside which the average density equals to the virial density ($\rho_{vir} = \delta_{th}\rho_M = \delta_{th}\rho_{cr} * \Omega_M$).

In order to be consistent of the simulation parameters, we take $\delta_{th} = 200$, Hubble constant $H_0 = 72kms^{-1}Mpc^{-1}$ for a flat universe, and $\Omega_M = 0.216$ for our cosmological model. With these standard parameters, r_{vir} is defined to be:

$$r_{vir} = 163h^{-1}kpc \left(\frac{\delta_{th}\Omega_M}{43.2}\right)^{-1/3} \left(\frac{M_{vir}}{10^{12}h^{-1}M_\odot}\right)^{1/3} \qquad (13)$$

Only two independent parameters, C and M_{vir}, need to be specified to define the values of all other halo quantities.

The reconstruction of the LMC's orbital parameters depends less sensitively on the Galactic mass distribution at distances much smaller than r_p where most of the baryonic matter resides. Nevertheless, we include the baryonic matter's contribution to the Galactic potential so that our model is self consistent, ie it can reproduce the observed circular velocity of the local standard of rest. The baryonic components include the mass of central black hole, the Galactic nucleus, bulge and an exponential disk with scale length r_d. We follow the equation outlined in Klypin et al. (2002) such that

$$M_b(r) = M_{BH} + 0.025M_{b,vir}[1 - exp(-2.64r^{1.15})]$$
$$+ 0.142M_{b,vir}[1 - (1+r^{1.5})exp(-r^{1.5})]$$
$$+ 0.833M_{b,vir}\left[1 - \left(1+\frac{r}{r_d}\right)exp\left(-\frac{r}{r_d}\right)\right](14)$$

The disk surface density is:

$$\Sigma(r) = \Sigma_0 \, exp\left(-\frac{r}{r_d}\right) \qquad (15)$$

where $M_{b,vir}$ is the total mass of the cooled baryons, as a fraction of the virial mass of dark matter halo, $M_{b,vir} = 0.05M_{vir}$ and $r_d = 3.5kpc$ is the scale length of the disk corresponding to the location of the Sun as $8.5kpc$. e.g. if $M_{vir} = 10^{12}M_\odot$, the total mass of the disk is $4.2 \times 10^{10}M_\odot$ and the bulge mass as $7.1 \times 10^9 M_\odot$.

Since the pericenter of the LMC's orbit is about $50kpc$, which is far away from the typical size of disk and bulge, the exact baryonic mass distribution is not very important for the orbital history, but it is relevant to the solar circular velocity. The rotation curve of an exponential disk is (Freeman 1970):

$$V_{disk}^2(r) = 4\pi G\Sigma_0(y)[I_0(y)K_0(y) - I_1(y)K_1(y)] \qquad (16)$$

where $y = r/r_d$ and I_n, K_n are the Modified Bessel Functions of the first and second kind(Binney & Tremaine
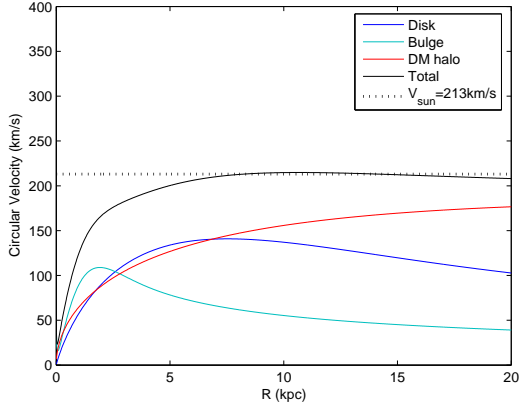
FIG. 3.— The rotation curve for $M_{vir} = 10^{12}M_{\odot}$, $R_{vir} = 200kpc$ and $C = 12$. The total potential gives $V_{c,sun} \sim 213 km s^{-1}$.
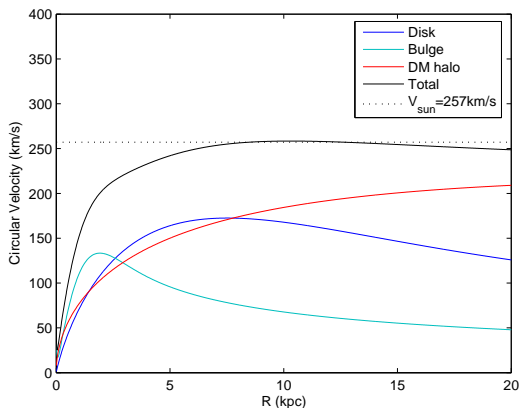

FIG. 4.— The rotation curve for $M_{vir} = 1.5 \times 10^{12}M_{\odot}$, $R_{vir} = 232kpc$ and $C = 13$. The circular velocity at $8.5kpc$ is $V_{c,sun} \sim 257 km s^{-1}$.

2008). The zero-pressure rotation velocity can be determined as:

$$V_c^2(r) = V_{disk}^2(r) + \frac{G}{r}[M_{BH} + M_{nul+bul}(r) + M_{halo}(r)] \tag{17}$$

Here we do not consider the adiabatic contraction of the dark matter halos.

With this velocity of the Sun, we can calculate the current velocity of LMC. If we choose M_{vir} to be of the order $10^{12}M_{\odot}$ or $1.5 \times 10^{12}M_{\odot}$, it self-consistently gives V_c of the Sun to be 220km s^{-1} or 250km s^{-1} respectively from the rotation curve (see Figs 3 and 4).

When we choose different parameters of NFW models to calculate the orbital history of LMC, the V_c will also be adjusted slightly according to the changing dark matter mass inside the location of the Sun.

4.2. *Simulated models of dark matter halo*

The NFW model is well suited for the part of the Galaxy within the virial radius. If we extrapolate this model for the entire dark matter halo, its density would decrease as $\rho \propto r^{-3}$ for $r >> r_s$. However, from the numerical simulations carried out by Oser et al.(2010), we find that the actual halo density profile is somewhat flatter than expected for the NFW model, ie there is more residual dark matter at large distance than that inferred from the NFW model. As we have discussed above, the LMC's orbital history is very sensitively determined by the density gradient of the outside part of the Galaxy. Here, we use a more realistic dark halo profiles which is extracted directly from the cosmological simulations.

In order to constrain the dark matter density profiles at large Galactocentric radii, we choose a set of 4 'zoom-in' cosmological simulations of individual halos (Oser et al. 2010). The initial condition of this simulation is based on a flat WMAP3 cosmology (Spergel et al. 2007) with model parameters: h=0.72, $\Omega_b = 0.044, \Omega_m = 0.216, \Omega_\Lambda = 0.74$ and $\sigma_8 = 0.77$. The initial slope of the power spectrum is $n_s = 0.95$.

At redshift zero we identify halos with the help of a friends-of-friends finder and choose relaxed halos with no massive companion close-by for re-simulation. We trace back in time all particles closer than two times the virial radius to the halo center in any given snapshot and replace those particles with multiple dark matter particles of lower mass while adding the small scale density fluctuations with the help of GRAFIC2 (Bertschinger 2001) The dark matter particles outside the region of interest are merged (depending on their distance to the re-simulated halo) to reduce the particle count and the simulation time. This way we are able to simulate structure formation in the cosmological context at high resolution in a reasonable amount of time. To evolve the high resolution initial conditions from redshift $z = 43$ to the present day we use the parallel Tree-code GADGET-2 (Springel 2005).

The set of 4 halos in Table 1 have masses in the range of $0.5 - 2 \times 10^{12}M_{\odot}h^{-1}$. The computational domain corresponds to a cosmic cube with the size of 100Mpc/h. The dark matter is represented by particles with a mass $2.5 \times 10^7 M_{\odot}h^{-1}$ and a comoving gravitational softening length of $890h^{-1}$ pc. The radial dark halo density structure is well resolved in the region from $r_p = 50$ kpc to the virial radius and beyond.

In order to apply the simulation data to the computation of the LMC's orbit, we first match the simulated dark matter distribution inside 200 kpc with NFW models to extract the best fitted values of ρ_s and r_s. Based on these two values, we then match the density distribution at around 200 kpc with the fitting formula

$$\rho = \frac{\rho_s}{(r/r_s)(1 + r/r_s)^\beta} \tag{18}$$

to determine the value of β. Instead of the idealized NFW profile in equation (8) which is equivalent to the case of $\beta = 2$, we use the above fitting procedures to approximate the dark matter halo's density profile beyond 200 kpc (see Table 1). In Figure 5, we show the LMC's orbital history for various model parameters. Since the M_{vir} values for these halos are relatively high and $\beta < 2$, it is possible for LMC to have more than one peri-galacticon passage even for $V_{sun} < 250km/s$. Note that there is one low-M_{vir} model (1167), where the LMC is undergoing its first peri galacticon passage.

In the results listed in Table 1, we also calculate the theoretical circular velocity of the Sun, in accordance with the Equations (16) and (17). The actual observed circular velocity at the Sun's location is related to the precise mass structure of the baryonic mass, because for
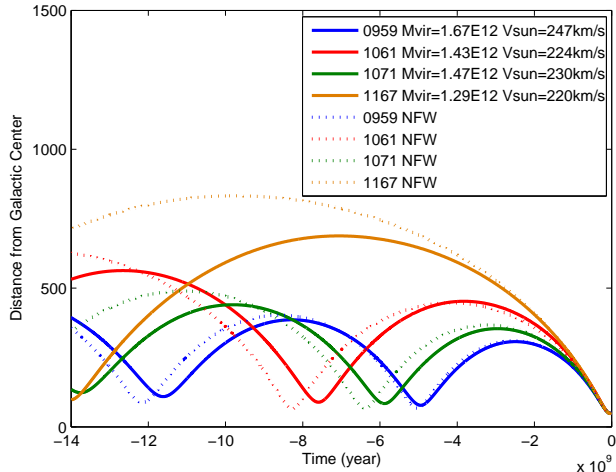
FIG. 5.— Orbital history of the LMC for simulated dark matter halos. The dark matter structure beyond $200kpc$ is determined from equation (18). The solid lines show the orbits for dark halos with β as given in Table 1. The dotted curves show the situation if one would take a dark halo with similar virial parameters but fixing beta at 2 as expected for an idealized NFW profile.

TABLE 1

data	$M_{vir}(10^{12}M_\odot)$	$r_{vir}(kpc)$	$r_s(kpc)$	β	V_c (km s^{-1})
0959	1.67	240	21	1.78	247
1061	1.43	228	18	1.61	224
1071	1.47	231	21	1.69	230
1167	1.29	221	21	1.83	220

From the simulation results of Oser, et al. (2010).

the inner part of the Galaxy, the contribution of circular velocity from the baryonic matter in the disk is comparable to that from dark matter (Fig 3 & 4). The theoretical model we used here for an exponential disk may lead to an underestimation of the Sun's circular velocity. Although the theoretical circular velocities for the models listed in Table 1 do not match exactly the latest observational data (ie $V_c \sim 254km/s$), the extra mass we need to make the velocity to be consistent with the observation is very small compared with the total mass within $50kpc$. Since the LMC does not venture into this inner region of the Galaxy during its orbital history, the precise structure inside $8.5kpc$ does not affect our determination of the LMC's orbital history.

The observationally determined values of V_c remain uncertain within the range between 220 km s^{-1} to 250 km s^{-1} (Reid et al. 2009a, Bovy et al. 2009, 2012, also see §1). If these values are applied to the NFW models, the lower limit of V_c would imply a single perigalacticon passage for the LMC whereas with the upper limit of V_c, the LMC would have had multiple perigalacticon passages. However, with the modified density distribution for the outer galactic halo, the LMC in three models (0959, 1061, and 1071) with $V_c > 228$ km s^{-1} have had multiple perigalacticon passages. Only in one model (1167) with $V_c = 221$ km s^{-1}, the LMC's orbital period is marginally smaller than 13 Gyr. Based on these results, we suggest if $V_c > 228$ km s^{-1}, LMC would likely have undergone more than one perigalacticon passages.
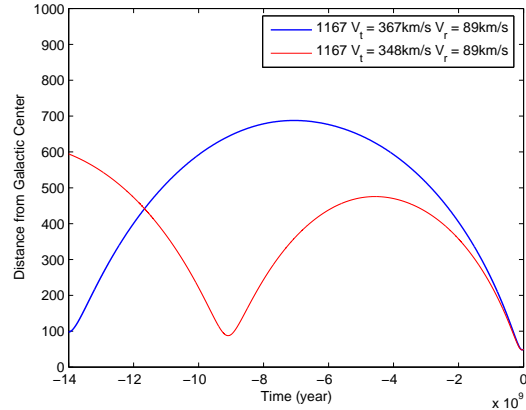
The correction resulting from the most recent observed

FIG. 6.— Orbital history of the LMC with the minimum transverse velocity $V_t = 348$ km s^{-1}. This value of V_t is within the error-bar from that $(V_t = 367$km s$^{-1})$ derived with $V_c = 220$km s^{-1}. For both cases, we used the same current radial velocity for the LMC as $V_r = 89$km s^{-1} and the halo potential in accordance to model 1167.

circular velocity of the Sun leads to a smaller transverse velocity, orbital period, and apo galacticon distance for the LMC (see §2). However, even without this change in the circular velocity of the Sun, the 1σ error bar in the LMC's observed velocity is ~ 18km s^{-1}. In order to assess the implication of these uncertainties on the LMC's orbital history, we use a range of transverse velocities of the LMC's current orbit that are consistent with the uncertainties in V_t of367 ± 18km s^{-1} and re-calculate the orbital history with the simulated halo based from the model 1167 which has $M_{vir} \sim 1.3 \times 10^{12}M_\odot$ and $R_{vir} \sim 220$kpc. In Figure 6, we show that the velocity uncertainties are large enough to introduce a significant modification in the LMC's orbital period as we have already suggested in §3.2. Although the mean and high values of the transverse velocity imply that the LMC has just passed through its perigalacton for the first time, the lowest value of the transverse velocity would imply a multiple peri galacticon passage for the LMC. This error analysis poses a challenge to the statistical significance of the single passage result obtained by Besla et al (2007).

4.3. Model including halo evolution

Since the LMC's orbital period is either comparable (in the case of a single passage) or a significant fraction (in the case of multiple passages) of the Hubble time, it is relevant to consider the evolution of the Galactic dark matter halo. However, the build up of the dark matter halo is a very complex process. It involves merger events, accretion and dynamical relaxation. In order to construct a model for the evolution of the Galactic halo, we need to identify the dominant mechanism.

We begin with an observational interpretation. The age of the thin Galactic disk can be traced by the age (> 10 Gyr) of old white dwarfs in it(Hansen et al. 2004). The preservation of the thin disk structure for this population of stellar remnants suggests that the Galaxy may have not had any major merger events during the past 10 Gyr. However, a significant mass increase due to a smooth infall or cold streams cannot be ruled out.

Another approach to model the evolution of the dark matter halo is to utilize the ΛCDM models which
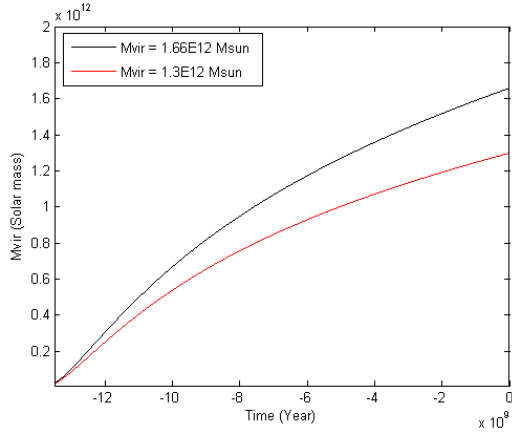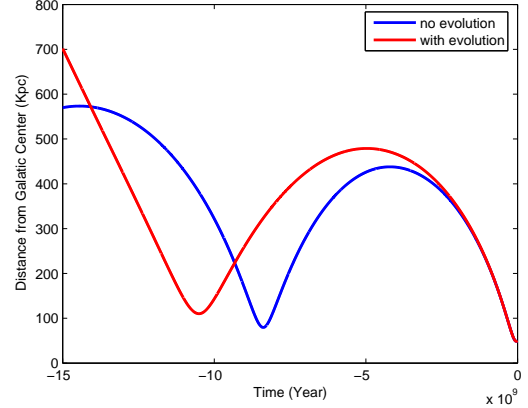
FIG. 7.— Mass evolution according to eq.(19).

FIG. 8.— Orbital history of the LMC with and without evolution of the dark matter halo. The concentration parameter is $C = 12$ as constant with the current $M_{vir} = 1.3 \times 10^{12} M_\odot$ and kept constant at a value of $R_{vir} = 221 kpc$. The corresponding circular velocity is $V_{sun} = 236$km s^{-1}.

were used to model the density distribution we used in §4.1. Here we adopt a recently developed prescription (Krumholz & Dekel 2012) based on the assumption that the in-streaming of baryonic and dark matter has led to the growth in the Galactic potential and the virial mass at a rate

$$\dot{M}_{vir,12} = -0.628 M_{vir,12}^{1.14} \dot{\omega} \qquad (19)$$

where $M_{vir,12} = M_{vir}/10^{12} M_\odot$. In the above equation, $\omega = 1.68/D(t)$ is the self-similar time variable of the extended Press-Schechter (EPS) formalism, and $D(t)$ is the linear fluctuations' growth function. Based on this EPS formalism, Neistein et al. (2006) and Neistein & Dekel (2008) estimate

$$\dot{\omega} = -0.0476[1 + z + 0.093(1+z)^{-1.22}]^{2.5} Gyr^{-1}. \quad (20)$$

The virial radius is related to both virial mass and redshift via $r_{vir} \propto M_{vir}^{1/3}/H(z)^{2/3}$ (Burkert et al. 2010), where $H(z)$ is:

$$H(z) = H_0[\Omega_\Lambda + (1 - \Omega_\Lambda - \Omega_M)(1+z)^2 + \Omega_M(1+z)^3]^{\frac{1}{2}}. \quad (21)$$

The redshift is also related to universal time through:

$$t = \frac{2}{3H_0\Omega_0^{1/2}(1+z)^{3/2}}. \qquad (22)$$

With these two relations, we can model the time evolution of the virial radius and calculate the orbital history of the LMC with this simplified evolution model for the dark matter halo.

We consider a low-mass (with the virial mass $M_{vir} = 1.3 \times 10^{12} M_\odot$) and a high-mass ($M_{vir} = 1.66 \times 10^{12} M_\odot$) case. These limits are comparable with the minimum and maximum masses of the simulation data. For both cases, we set the concentration parameter $C = 12$ and neglect its evolution. For these two sets of model parameters, the initial mass accretion rate is relatively high ($> 100 M_\odot$ yr^{-1}) at redshift $z > 2$(Fig.7). Although in the evolutionary models, M_{vir} increased steadily LMC's orbits since the previous perigalacticon passage for the evolutionary models are similar to those with a fixed halo. For the low mass model (Fig. 8), the previous apo and perigalacticons occurred at 4 and 8 Gyr ago when M_{vir} has already attained 85% and 50% of its value at $z = 0$

respectively. The late mass increase of the halo potential does not modify LMC's orbit significantly. However more than 10Gyr ago, M_{vir} was substantially smaller than today. The play back integration of LMC's orbits for the evolving and the non evolving halo models therefore diverges at high redshift. This divergence is similar to that between models which include or neglect contributions from dynamical friction. However the dynamical friction effect decreased at early epochs in the evolving halo model due to a decreased density of dark matter back then.

Similar results are also obtained for the high mass model (Fig. 9). In this case, the previous apo and perigalacticons occurred at 1.8 and 3.6 Gyr ago when M_{vir} has already attained 94% and 88% of its value at $z = 0$. Thus, the divergence between the orbits for the evolving and non evolving dark matter halo is only significant more than 8 Gyr ago, when the LMC passed through two peri galacticon passages prior to the present epoch. We note that when the evolution of the halo is taken into account, the number of passages declines by at most one in comparison with that for the non evolving halo.

In the above models, we adopt a constant concentration parameter. For an alternative possibility, we consider a model in which C increased linearly from $C = 4$ to $C = 12$ during cosmic time for the evolving halo models. We consider the case with the asymptotic virial mass $M_{vir} = 1.66 * 10^{10} M_\odot$ (see Fig.10). The small concentration at early time makes the LMC's orbit more loosely bound. However, in comparison with the non-evolving halo model (with a fixed $C = 12$), the difference results from C variations is not very significant. It seems that the orbital period of LMC is more dependent on the current concentration of the dark matter halo than the initial value.

5. SUMMARY

Besla et al (2007) utilized LMC's three dimensional velocity data to reconstruct LMC's orbital history. They made a bold suggestion that the LMC has passed the perigalacticon of its Galactic orbit for the first time. This conclusion, if it can be verified, would invalidate the tidal disruption hypothesis for the Magellanic Stream.
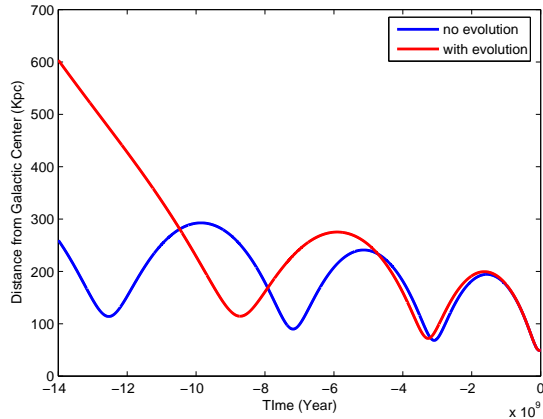
FIG. 9.— Orbital history of the LMC with and without the evolution of a larger dark matter halo. The concentration parameter is $C = 12$ and constant with the current $M_{vir} = 1.66 * 10^{12} M_{\odot}$ and $R_{vir} = 240kpc$. The corresponding circular velocity is $V_{sun} = 259$km s^{-1}.
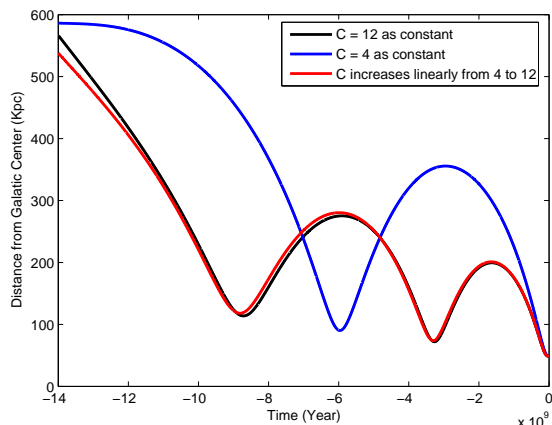

FIG. 10.— Orbital history of LMC with linear evolution of concentration parameter of DM halo, compared to the results with fixed $C = 12$ and $C = 4$. The final mass is $M_{vir} = 1.66 \times 10^{12} M_{\odot}$.

We show that these previous results depend critically on the LMC's transverse velocity and the dark matter distribution in the outer Galactic halo. At the LMC's latitude and longitude in the sky, a large fraction of its observed proper motion is due to the Sun's circular velocity around the Galactic center. We use the most recently measured solar circular velocity (254 km s^{-1}) rather than its conventional value (220 km s^{-1}) to deduce a smaller transverse speed, apogalacticon distance, and orbital period for the LMC. It raises the possibility that the LMC actually had two or more previous perigalacticon passages.

We adopt the current velocity of LMC with a different solar velocity, and a simply modeled potential profile of the Milky Way outside 50kpc to examine its orbital history. We find that the number of passages depends sensitively on the slope of the potential and density distribution of the dark matter halo as well as the current transverse velocity of LMC near its perigalacticon distance.

With an illustrative model (in Fig. 2), we show that, for a relatively flat Galactic potential (with lambda=0.1), a modest (7 percent) decrease in the deduced value of V_t can lead to a much larger (30 percent) decline in the LMC's inferred orbital period. Thus, a precise determination of LMC's orbital history can provide a sensitive measurement on the distribution of dark matter halo in the extended outer regions of the Milky Way Galaxy.

In this paper, we have neglected the perturbation on the LMC from any other member of Local Group, including M31. If we choose a massive model of dark matter halo ($M_{vir} = 1.66 \times 10^{12} M_{\odot}$), the pericenter's location of the last two orbital periods would be well within $400kpc$ (Fig.9). The current distance between M31 and the Milky Way is about $700kpc$, it was even further away in the past since they are currently approaching each other. The M31-Galaxy orbital plane also appears to be inclined to the LMC-Galaxy orbital plane. It's perturbation on the previous the LMC's orbital history appear to be weak. This assumption is also consistence from the lack of warp along the great circle which is traced out by the Magellanic Stream. Nevertheless, a more comprehensive set of simulations is needed to justify the dynamic independence between M31 and the Milky Way galaxies.

7. REFERENCE

Besla, G., Kallivayalil, N., Hernquist, L., Roberston, B., Cox, T. J., van der Marel, R. P., & Alcock, C. 2007, ApJ, 668, 949

Besla, G., Kallivayalil, N., Hernquist, L., van der Marel, R. P., Cox, T.J., & Keres, D. 2010, ApJL, 721, L97

Bertschinger, E. 2001, ApJS, 137, 1

Binney, J., Tremaine, S. 1987, Galactic Dynamic, (Princeton, NJ; Princeton University Press)

Binney, J., & Tremaine, S. 2008, in Galactic Dynamics, Second Edition (Princeton, NJ: Princeton Univ. Press), 390

Bovy, Jo, Hogg, David W., Rix, Hans-Walter 2009, ApJ, 704, 1704

Bovy, Jo, Prieto, C.A., Beers, T.C., Bizyaev, D., da Costa, L.N., Cunha, K., Ebelke, G.L., Eisenstein, D.J., Frinchaboy, P.M., Pere, A.L.G., Girardi, L., Hearty, F.R., Hogg, D.W., Holtzman, J., Maia, M.A.G., Majewski, S.R., Malanushenko, E., Malanushenko, V. , M esza r, S., Nidever, D.L., OConnell, R.W., ODonnell, C., Oravetz, A., Pan, K., Rocha-Pinto, H.J., Schiavon, R.P., Schneider, D.P., Schultheis, M., Skrutskie, M., Smith, V.V., Weinberg, D.H., Wilson, J.C., & Zasowski, G. 2012, ArXiv:1209.0759

Burkert, A., Genzel, R., Bouch, N., Cresci, G., Khochfar, S., Sommer-Larsen, J., Sternberg, A., Naab, T., Forster Schreiber, N., Tacconi, L., et al. 2010, ApJ, 725, 2324

Chandrasekhar, S. 1943, ApJ, 97, 255

Dehnen,W., & Binney, J. J. 1998, MNRAS, 298, 387

Fellhauer, M., Lin, D. N. C. 2007, MNRAS, 375, 604

Freeman, K. C. 1970, ApJ, 160, 811

Fujimoto, M., Sofue, Y. 1976, A&A, 47, 263

Gardiner, L. T., Sawa, T., Fujimoto, M. 1994, MNRAS, 266, 567

Gunn, J. E., Gott, J. Richard, III 1972, ApJ, 176, 1

Hansen, Brad M. S., Richer, Harvey B., Fahlman, Greg. G., Stetson, Peter B., Brewer, James, Currie, Thayne, Gibson, Brad K., Ibata, Rodrigo, Rich, R. Michael, Shara, Michael M. 2004, ApJS, 155, 551

Hashimoto, Y., Funato, Y., & Makino, J. 2003, ApJ, 582, 196

Jones, B. F., Klemola, A. R., Lin, D. N. C. 1994, AJ, 107, 1333

Kahn, F. D., Woltjer, L. 1959, ApJ, 130, 705

Kallivayalil, N., van der Marel, R. P., Alcock, C., Axelrod, T., Cook, K. H., Drake, A. J., Geha, M. 2006, ApJ, 638, 772

Kallivayalil, N., van der Marel, R. P., Alcock, C. 2006, ApJ, 652, 1213

Klypin, A., Zhao, H., & Somerville, R. S. 2002, ApJ, 573, 597

Krumholz, M. R. & Dekel, A. 2012, ApJ, 753, 16

Lin, D. N. C., Jones, B. F., Klemola, A. R. 1995, ApJ, 439, 652

Lin, D. N. C., Lynden-Bell, D. 1982, MNRAS, 198, 707

Lynden-Bell, D., Lin, D. N. C. 1977, MNRAS, 181, 37

Majewski, S. R., Skrustkie, M. F., Weinberg, M. D., & Ostheimer, J. C. 2003, ApJ, 599, 1082

Mastropietro, C., Moore, B.; Mayer, L., Stadel, J. 2005, ASPC, 331, 89

Mathewson, D. S., Cleary, M. N., & Murray, J. D. 1974, ApJ, 190, 291

Meatheringham S.J., Dopita M.A., Ford H.C. & Webster B.L. 1988, ApJ, 327,651

Mirabel, I. F., Turner, K. C. 1973, A&A, 22, 437

Moore, B., Davis, M. 1994, MNRAS, 270, 209

Murai, T., Fujimoto, M. 1980, PASJ, 32, 581

Navarro, J. F., Frenk, C. S., White, S. D. M. 1997, ApJ, 490, 493

Neistein, E., & Dekel, A. 2008, MNRAS, 383, 615

Neistein, E., van den Bosch, F. C., & Dekel, A. 2006, MNRAS, 372, 933

Oser, L., Ostriker, J.P., Naab, T., Johansson, P.H. & Burkert, A. 2010, ApJ, 725, 2312

Peebles, P. J. E. 2001, ASPC, 252, 201

Peebles, P. J. E. 2010, arXiv:1009.0496

Putman, M. E., Gibson, B. K., Staveley-Smith, L. 1999, ASPC, 165, 113

Reid, M. J., Menten, K. M., Zheng, X. W., Brunthaler, A., Moscadelli, L., Xu, Y., Zhang, B., Sato, M., Honma, M., Hirota, T. et al. 2009a, ApJ, 700, 137

Shattow, G. & Loeb, A. 2009, MNRAS, 392, L21.

Spergel, D. N., Bean, R., Dor, O., Nolta, M. R., Bennett, C. L., Dunkley, J., Hinshaw, G., Jarosik, N., Komatsu, E., Page, L., et al. 2007, ApJS, 170, 377

Springel, V., Yoshida, N., & White, S. D. M. 2001, New Ast., 6, 79

Springel, V., Yoshida, N., & White, S. D. M. 2005, MNRAS, 364, 1105

Toomre, A., 1972, QJRAS, 13, 266

van der Marel, R. P., Alves, D. R., Hardy, E., Suntzeff, N. B. 2002, AJ, 124, 2639

van der Marel, R. P., Fardal, M., Besla, G., Beaton, R. L., Sohn, S. T., Anderson, J., Brown, T., Guhathakurta, P. 2012, ApJ, 753, 8